Journal of Geoscience and Environment Protection, 2022, 10, 229-256
https://www.scirp.org/journal/gep
ISSN Online: 2327-4344
ISSN Print: 2327-4336

Conceptual Model of Aquifers in the Bedrock Zone of the Marahoué Watershed (Centre-West of Ivory Coast)

Kouassi Désiré Bouatrin*, Innocent Kouassi Kouame, Aristide Gountôh Douagui, Kouamé Auguste Kouassi, Bi Tié Albert Goula

Geosciences and Environment Laboratory, Department of Environmental Sciences and Management, Nangui University Abrogoua, Abidjan, Ivory Coast
Email: *bouatrin.kd@gmail.com, innocent_kouassi@yahoo.fr, douaguiaristide@yahoo.fr

How to cite this paper: Bouatrin, K. D., Kouame, I. K., Douagui, A. G., Kouassi, K. A., & Goula, B. T. A. (2022). Conceptual Model of Aquifers in the Bedrock Zone of the Marahoué Watershed (Centre-West of Ivory Coast). *Journal of Geoscience and Environment Protection, 10,* 229-256.
https://doi.org/10.4236/gep.2022.107014

Received: April 8, 2022
Accepted: July 24, 2022
Published: July 27, 2022

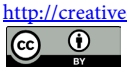

Abstract

Marahoué watershed, located in the Center West of Côte d'Ivoire, has experienced significant population growth in recent decades. And a major economic boom linked to intense agricultural activity and the presence of certain industries. This population growth is also accompanied by seasonal water shortages. Hence it needs to better manage the basin's groundwater, which is a permanent resource and more resistant than surface water to climatic hazards. The objective of this study is therefore to propose a conceptual model of hydrogeological flow for the sustainable exploitation of groundwater resources in the Marahoué watershed. The establishment of the conceptual model was carried out in two stages. The first step consisted in defining the stratigraphic units. For this purpose, three units have been defined. These are the layer of alterite, the useful fissured horizon and the sound basement. The thickness of the layer of alterite varies from 0 to 80 m with an average of 26 m. As for the useful fissured horizon, its thickness is between 43 and 46.5 with an average of 45 m. In addition, the roof of the basement presents a slightly uneven morphology with a North-West, South-East dip and the altitudes are between 150 and 390 m. The second step corresponds to the phase of determining the hydrodynamic parameters. During this phase, the crack porosity, the transmissivity, the conductivity, the storage coefficient, the hydrological balance and the piezometric map were determined. Indeed, these parameters (the crack porosity, the transmissivity, the conductivity and the storage coefficient) confirm not only the heterogeneity of the medium but that the cracked horizon is sufficiently porous to be assimilated to an equivalent continuous medium during the simulation.

Keywords

Marahoué Watershed, Conceptual Model, Ivory Coast

1. Introduction

In Africa, particularly in West Africa, the decline in the level of rainfall, environmental degradation and population growth have caused a depletion of water resources (Baron & Bonnassieu, 2011; Mahé et al., 2001). One of the major consequences of the fall in rainfall is the increasing reduction in groundwater recharge (Ouedraogo, 2016). However, nearly half of Africa's population relies on groundwater, which in many rural areas of sub-Saharan Africa is the only sustainable source of water for human consumption (Carter & Parker, 2009).

Marahoué watershed, located in the center west of Côte d'Ivoire in the basement zone (Biémi, 1992; Akpo et al., 2016; Irie et al., 2015), is also affected by this drop in rainfall. The populations who live there frequently experience a shortage of drinking water during the dry seasons, accentuated by untimely water cuts by SODECI (Water Distribution Company in Côte d'Ivoire) for up to two weeks or even a month or more in some localities. This shortage is accentuated in the villages and camps which lack village pumps. This problem can be attributed to the fact that there is a significant increase in bare soils/habitats and crops while the water reservoirs are strongly regressing (Irie et al., 2015). Also added is the fact that the productivity of boreholes is difficult to predict in the basement zone (Lachassagne et al., 2015; Ouedraogo, 2016; Yao, 2011). This causes several failures during the construction of hydraulic structures for groundwater catchment in particular (wells and boreholes), structures that are essential for the permanent supply of drinking water to the populations. Thus, the increasingly strong social demand makes it necessary to elucidate the major questions that arise for both researchers and managers in order to better understand the mechanisms conditioning the availability and distribution of groundwater for better management of this resource. We can only manage well what we know well.

The models can thus serve as a basis for decision-making in a resource management framework. They are also a tool for improving the understanding of underground hydrodynamic phenomena (Jaunat, 2013). In addition, the conceptual model schematically describes the studied aquifer system (Kouamé, 2007). It specifies the horizontal and vertical extension, details the succession of aquifers and aquitards, describes the lithology and the dominant hydrogeological characteristics, explains the hydraulic conditions at the limits of the system, evaluates the main components of the flows passing through it and identifies the zones of recharge and outlet (Barthélemy & Seguin, 2016).

Indeed, basement aquifers are made up of crystalline rocks, of plutonic (granites) and metamorphic (gneiss, schists, micaschists, etc.) origin. Hydrogeologi-

cally, it is hard rock ("hard rock" in English) (Lachassagne et al., 2015). They thus exhibit, despite very diverse origins and compositions, a relatively homogeneous overall behavior and similar properties. They are mainly characterized by permeability of cracks and fractures. The aquifers they contain are therefore classically considered as discontinuous, due to the significant spatial variability of their hydrodynamic properties (Lachassagne et al., 2005). Between the sound impermeable rock and the surface alterites, there is an intermediate horizon called the fissured horizon. Unlike alterites, this environment has high permeability and forms the transmissive part of the aquifer (Duran, 2005). To this end, the knowledge, at the scale of the watershed, of the geometry (roof, wall) and of the hydrodynamic properties of the two main constituent horizons of the bedrock aquifer makes it possible to define its underground water reserve (Lachassagne et al., 2015). Thus, faced with this seasonal water shortage, a conceptual model of hydrogeological flows is required in the Marahoué watershed.

It is in this context that this study was initiated, the objective of which is to propose a conceptual model of hydrogeological flow for the sustainable exploitation of groundwater resources in the Marahoué watershed. This will first involve defining the stratigraphic units and then determining the hydrodynamic input parameters of the flow model.

2. Materials and Methods

2.1. Study Zone

Marahoué River watershed is a sub-basin of the Bandama River watershed which has an area of 97,000 km^2, or about 30% of the area of Côte d'Ivoire (Avenard et al., 1971; Kamagate et al., 2011). It is located between longitude 5˚31'80.0" and 7˚1'80.0" West and latitude 6˚45'60.0" and 9˚27'0.0" North. Its area is 24,300 km^2. From an administrative point of view, the watershed of the marahoué straddles six (6) regions (Béré, Worodougou, Marahoué, Bagoué, Haut Sassandra and Kabadougou). 550 km long, the main river (the Marahoué) is flanked by two tributaries: the Béré to the east and the Yani or Bahoroni to the west (Irie et al., 2016; Biémi, 1992). In fact, the Marahoué watershed straddles two climatic regimes. In the north, we distinguish the subtropical regime (Sudanese climate) and in the south the humid tropical regime (Baouléan climate) (Goula et al., 2006). The subtropical regime is characterized by two seasons, a rainy season from May to October (6 months) and a dry season from November to April (6 months) which is accentuated by the harmattan with lower average annual rainfall (1977-2001) at 1200 mm. The humid tropical regime is distinguished by a four-season climatic regime and average annual rainfall (1977-2001) which varies on average between 1200 mm and 1600 mm. Namely, a long rainy season from March to June (4 months), a short dry season from July to August (2 months), a short rainy season starting in September and ending in October (2 months) and a great dry season from November to February (4 months) (Irié, 2019).

Geologically, several types of petrographic facies have been identified (Figure 1). These are fine-grained granite, porphyroid granite with biotite and dominant pink feldspar, biotite granite with migmatitic and gneissic past, granodiorite, migmatites, eyed gneiss, volcano-sedimentary and detrital rocks, vein complexes (Biémi, 1992). These geological formations are grouped into two main entities: magmatic rocks and metamorphic rocks.

2.2. Setting up the Conceptual Model

The purpose of setting up the conceptual model is to simplify the system to be modeled and to organize the associated data to take them into account in a numerical model (Koffi, 2004). According to Anderson and Woessner (1992), the essential steps in setting up the conceptual model are the definition of the hydrostratigraphic units and the preparation of the water balance.

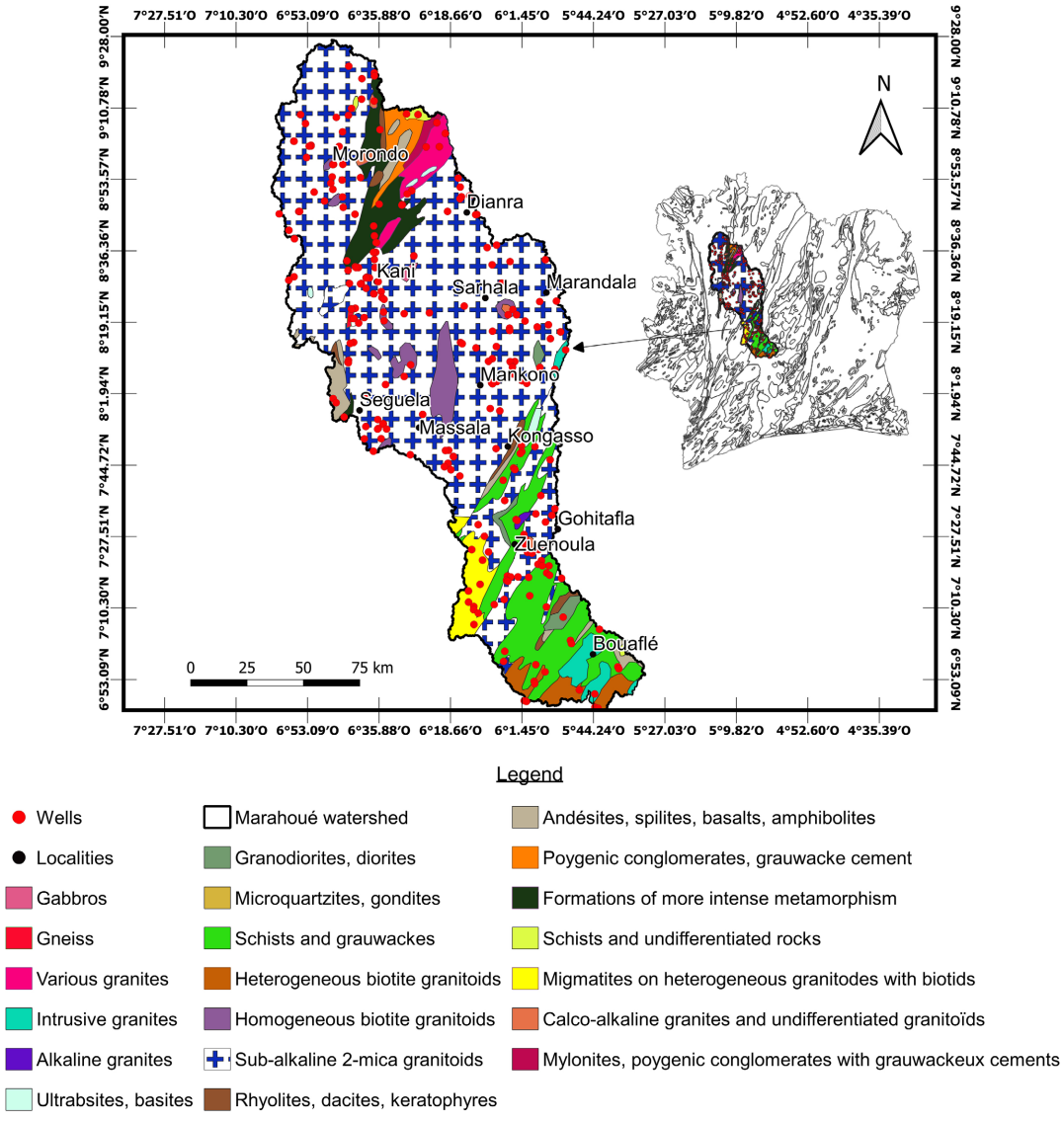

Figure 1. Marahoué watershed (excerpt from the geological map of Côte d'Ivoire) (Delor et al., 1995).

2.2.1. Development of the Digital Terrain Model (DTM)

The DTM file of the Marahoué watershed was set up using radar images captured from February 11 to 22, 2000 during the Shuttle Radar Topography Mission (SRTM) and published in September 2014. These are scenes n06_w006_1arc_v3, n06_w007_1arc_v3, n07_w006_1arc_v3, n07_w007_1arc_v3, n08_w006_1arc_v3, n08_w007_1arc_v3 n08_w008_1arc_v3, n09w007_1arc_v3. This SRTM 1 Arc-Second elevation data provides worldwide coverage with a resolution of one (1) arc second (30 meters) and provides the global dataset. Also, the DEM file was made in three (3) steps. The first step concerns the acquisition of the different scenes. Access to these data was possible thanks to the Earth Explorer software, developed by the USGS (United States Geological Survey). This application was used to search, preview and download SRTM 1 Arc-Second Global elevation data. After the downloads, the next step is the processing phase. This phase consisted of mosaicking the different scenes with the SNAP software. Finally, the last step was devoted to extracting the contour of the Marahoué watershed from these different scenes and then coloring the different altitudes with the QGIS 3.16.2 software. This approach allowed the final implementation of the DTM of the basin.

2.2.2. Layers Model Design

The design of the layer model was carried out from sections of boreholes collected in the various Territorial Directions of Hydraulics (DTH) of the Marahoué watershed. These are the DTHs of Daloa; puffed up; Seguela; Mankono and Boundiali. Cross-checking of the geological profiles of the various boreholes at the longitudinal and transverse level, based on the analysis of the technical data sheets, made it possible to identify and describe the formations present. The last water inflows were considered as the lower limits of the different fissured horizons at the level of the boreholes. Boreholes F1 to F11 (**Figure 2**) respectively of M'Bia; Morondo; Manabri; Silakoro; Lenguekro 2; flash; gohitre; Drikouafla 2; Djessikro; Gobazra Dioula and Seitinfla were used for the realization of the longitudinal profile (the North-West, South-East direction). Similarly, boreholes F12 to F16 (**Figure 3**) respectively from Sanankoro; N'gokro; _ Meneni; Korosso; Brokodalah were used for the realization of the transverse profile (the East – West direction).

2.2.3. Alterite Thickness Mapping

The weathering profiles manifested as two horizons, surface weathering and an underlying fissured horizon. If we assume that the thickness of the fissured horizon under the transition level with the alterites is almost constant spatially, we can then consider that it suffices to locate the contact zone of the alterites/fissured horizon to map the thicknesses of weathering profiles (Durand et al., 2015). Mapping the contact zone between the alterites and the fissured horizon consists in tracing the outline of the alterite outcrops as a lithological formation in itself. The mapping of the thickness of the alterites was carried out in two stages.

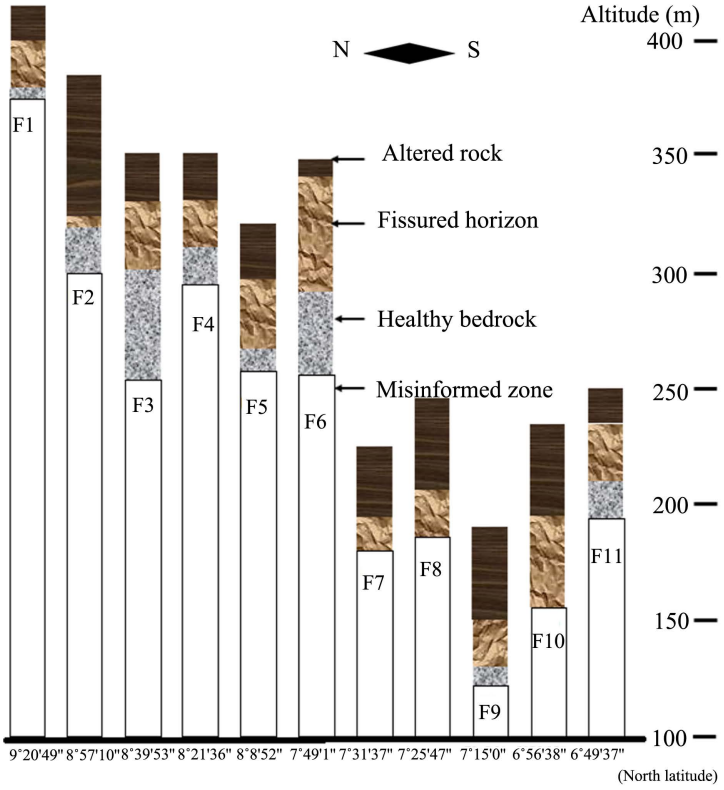

Figure 2. Longitudinal section of boreholes in the Marahoué watershed.

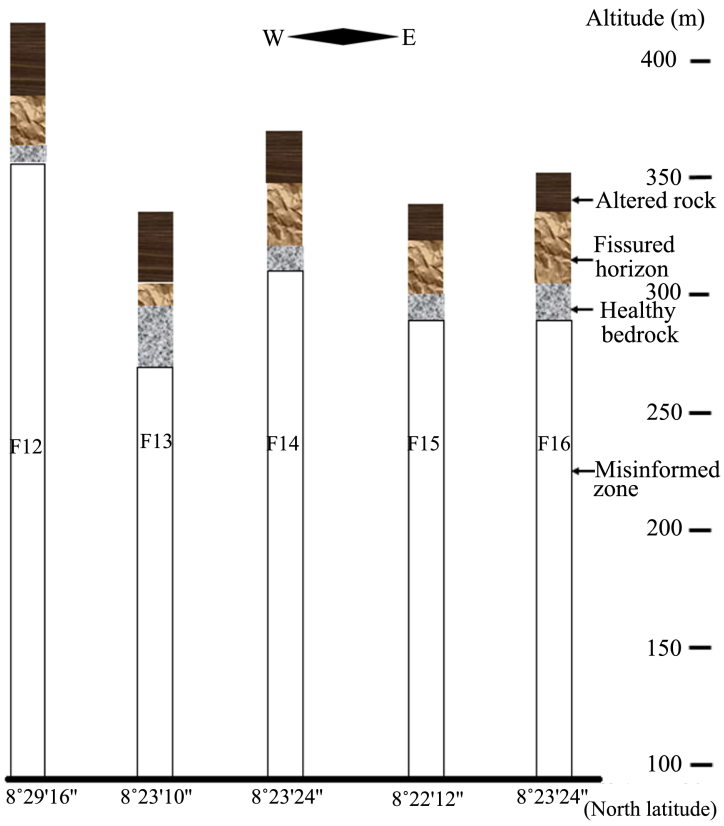

Figure 3. Cross section of boreholes in the Marahoué watershed.

The first step consisted in subtracting the level of alterites from the altitude (Z) of the 300 boreholes used here as observation points of the interface alterites/fissured medium. These levels of alterites generated, made it possible to construct by kriging the map of the interface alterites/fissured medium thus representing the roof of the basement. Then, the second step was devoted to the deduction of the thickness of the alterites at all points of the Marahoué watershed. To this end, it suffices to subtract the roof of the basement from the topographic altitude in the zones where the alterites are still in place to know the thickness of these at each point. For this, the DTM established is used under a Geographic Information System. On a new grid identical to that of the interpolation map, the value of the topographic altitude (DTM) removed from the altitude of the base of the alterites (roof of the base) is calculated using the raster tool ARCGIS 10.2 software calculator. Positive values, less than or equal to 80 m, are interpreted in terms of the thickness of the weathering layer. As for values greater than 80 m, they have been placed in the blank area of the map. In reality, beyond 80 m, the thickness of the layer of alterite coincides with the sectors where the slopes of the DTM were greater than 2%, which is higher than the limit commonly accepted by geologists as allowing the maintenance in place of altered formations on the plateaus (Mougin et al., 2015). With regard to the negative values (or the topographic surface which is located below the level of the base of the alterites), they give in absolute value the incised depth within the fissured horizon.

2.2.4. Helpful Fissured Horizon Mapping

The thickness of the fissured horizon was determined from linear flow rates (Q/P). By definition, the linear flow (Q/P) is the flow at the blowing of the boreholes (air lift flow noted Q) in relation to the depth (P) of the borehole (Equation (1)) under the base of the loose alterites (Lachassagne et al., 2015). The linear flows were calculated at the level of the three hundred (300) boreholes. Concretely, the method chosen for the determination of the thickness of the fissured horizon, is that which was developed by Courtois, entitled "80% percentile". It consists of calculating a cumulative percentage of linear flow (Courtois et al., 2008). This percentage makes it possible to deduce two values:

- First the thickness of the useful cracked horizon (L_u) which corresponds to the thickness defined by the threshold of 80% of the cumulative percentage of linear flow.
- Then the flow rate of this useful fissured horizon (Q_{Lu}) obtained by multiplying the flow rate of the useful fissured medium (average of the linear flow rates not in relation to the total number of boreholes) (Q_{pl}) and the thickness of the useful fissured horizon (Equations (2) and (3)).

The map of the thickness of the useful fissured horizon was carried out on the two geological formations, essential to the basin. That is to say on granites and schists. In total, 88.33% (i.e. 265) of the drillings were carried out on granites. The remaining 11.67% of the boreholes (i.e. 35 boreholes) were drilled on shales.

$$Q/P' = \frac{Q}{P} \tag{1}$$

$$Q_{pl} = \sum_{i=1,\cdots,n}^{L_u} \left(\frac{Q}{P_i'}\right) \Big/ Nf \tag{2}$$

$$Q_{Lu} = Q_{pl} \times L_u \tag{3}$$

With Q/P' the instantaneous linear flow and Nf the number of boreholes.

2.2.5. Determination of Hydrodynamic Parameters

The data used to determine the porosities, transmissivities, hydraulic conductivities and storage coefficients are the data from the 106 pumping test sheets collected in the various Territorial Hydraulics Departments (DTH) in the basin. Thus, the model adopted for determining the porosity of cracks is the Warren and Root model, also called the Double porosity model (Thiery et al., 1982; Koïta, 2010). According to Warren and Root the aquifer system is characterized by two factors. These are the ratio (F) and the interporosity flow parameter (ε). The ratio F is the ratio of the product of the porosity by the compressibility of the fractures compared to the product of the porosity by the compressibility of the system (Equation (4)). The ratio F (Equation (6)) is also determined by plotting the curve of the drawdowns as a function of time in semi-logarithmic coordinates. Then, one determines the porosity (ϕ_F) after having chosen the Coefficient of compressibility of water and that of compressibility of the matrix (Faillat et al., 1998; Thiery et al., 1982). Thus the ratio F is established as follows:

$$F = \frac{\phi_F C_e}{\phi_F C_e + (1-\phi_F) C_{ma}} \tag{4}$$

From Equation (4) we get the crack porosity ϕ_F

$$\phi_F = \frac{FC_{ma}}{C_e + FC_{ma} - FC_e} \tag{5}$$

$$F = 10^{\frac{-\Delta_S}{C}} \tag{6}$$

With

ϕ_F Porosity of fractures and connected pores;

C_e: Water compressibility coefficient;

C_{ma} Matrix compressibility coefficient.

Precise studies have made it possible to draw up the values of C_{ma} according to the rock matrix and of C_e according to the temperature of the water (**Table 1**). Under usual conditions, the temperature of water deposits is around 30˚C (Thiery et al., 1982). The corresponding coefficient of compressibility of water is close to $C_e = 4.6\times10^{-5}\ \mathrm{m^3/m^3/bar}$ either $C_e = 4.508\ \mathrm{m^2/kg}$.

The transmissivities were determined using the Cooper-Jacob (1946) method. Indeed, the method of the rise of Cooper-Jacob allows the calculation of the transmissivity (T) by interpretation of the equation of THEIS -JACOB with the following data:

Table 1. Values of the rock matrix compressibility coefficient used.

Nature of the rock matrix	C_{ma} in $m^3/m^3/bar$	C_{ma} in m^2/kg
granite	42×10^{-7}	4.116×10^{-10}
Sandstone	31×10^{-7}	3.038×10^{-10}
Shale	80×10^{-7}	7.82×10^{-10}

- $t_{i,s}$ time elapsed from the start of pumping until it stops;
- t' time counted after this stop;
- s' continuation of the recording of the drawdown in the control piezometer;
- Q pumping flow rate value that created the initial drawdown.

The mathematical reasoning for determining the effects of stopping pumping is based on the principle of superposition. A "fictitious continuation" of the pumping at the initial flow rate Q is combined with a "fictitious injection" of water at the same flow rate, i.e. pumping at the flow rate $-Q$. The drawdown is measured in the observation piezometer. Jacob then becomes:

$$s' = \frac{2.3}{4\pi} \cdot \frac{Q}{T} \cdot \log\left(\frac{2.25T \cdot (t_a + t')}{r^2 S}\right) - \frac{2.3}{4\pi} \cdot \frac{Q}{T} \cdot \log\left(\frac{2.25T \cdot t'}{r^2 S}\right) \quad (7)$$

$$s' = \frac{2.3}{4\pi} \cdot \frac{Q}{T} \cdot \log\left(\frac{t_a + t'}{t'}\right) \quad (8)$$

The calculation is done on a semi-logarithmic graph. The experimental curve of the test is drawn with $\frac{t_a + t'}{t'}$ (in fact $\log\left(\frac{t_a + t'}{t'}\right)$) in abscissa and ordinate (Assemian, 2014). Normally, all points tend to line up on a straight line. The slope of the line is obtained by doing:

$$\frac{\mathrm{d}s}{\mathrm{d}\log\left(\frac{t_a + t'}{t'}\right)} = \Delta s' = \frac{2.3}{4\pi} \cdot \frac{Q}{T} \quad (9)$$

with $\Delta s'$ slope. That is, the drawdown corresponding to one (1) logarithmic cycle.

We then obtain

$$T = \frac{2.3}{4\pi} \cdot \frac{Q}{\Delta s'} \quad (10)$$

The storage coefficient (S) is defined by Equation (11) (Thiery et al., 1982; Suski, 2006; Fouché, 2013):

$$S = \rho_w \cdot g \cdot (\phi_F C_e + C_{ma}) \times e \quad (11)$$

ϕ_F : Porosity of fractures and connected pores;

C_e: Water compressibility coefficient;

C_{ma}: Coefficient of compressibility of the matrix (deduced starting from **Table 1**);

e: the thickness of the aquifer (m);

ρ_w = density of water, 1000 kg/m^3;

g = gravitational acceleration ≈ 10 m/s^2.

Permeability (or hydraulic conductivity) is the ability of a reservoir to allow water to pass through under the effect of a hydraulic gradient. It expresses the resistance of the environment to the flow of water passing through it. It is determined from the transmissivity formula (Savané et al., 1997; Assemian, 2014).

$$T = K \cdot e \tag{12}$$

With "K" the Hydraulic conductivity in m/s

"e" the thickness of the aquifer in m.

"K" then becomes:

$$K = \frac{T}{e} \tag{13}$$

The thickness of the fractured zone is assimilated to the length of the strainer if the borehole has a single water inlet. If the borehole has several water inlets, the thickness of the fractured zone is determined by making the difference between the first water inlet and the last (Kouassi et al., 2013). The permeability values are classified according to the table of Castany (1982).

2.2.6. Determination of the Initial Piezometry of the Marahoué Watershed

This choice is justified by the fact that it was during this year that there was a maximum of boreholes (20 boreholes) made in the middle of the dry season (**Figure 4**). In reality, during the dry season, the groundwater that flows through

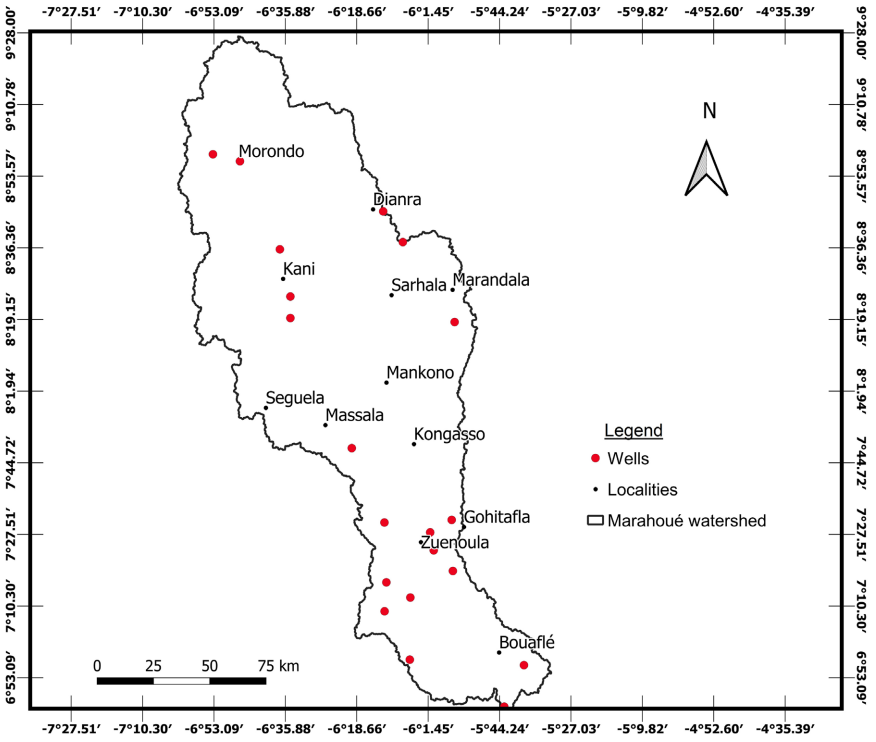

Figure 4. Distribution of boreholes used as piezometers.

the pores of the formation to the lower areas is not replaced by infiltrating rainwater. This promotes a better appreciation of the direction of groundwater flow in the basin (Soro, 2017). Piezometric levels are obtained from manually measured water depths according to Equation (14) (Yao et al., 2015)

$$Np = Z_{TN} - N_{mesure} + H_d \quad (14)$$

With Np: the piezometric level (m) referring to the edge of the casing,
Z_{TN}: the altitude (m) of the natural terrain at the location of the structure,
N_{mesure}: the depth (m) of the water surface measured with the probe and
H_d: the height (m) of the casing above ground.

2.2.7. Establishment of the Hydrological Balance

NASA Power meteorological data from 1987 to 2017 were used to establish the water balance of the Marahoué watershed. These data offer an advantage from the point of view of representativeness; spatiality and punctuality of measurements (Boudevillain, 2003). However, they require validation before any use. For this purpose, data from satellite measurement points close to the Bouaflé rainfall stations; Mankono; Séguéla and Boundiali were used. These data were compared to the terrestrial data of the cities mentioned above for the period from 1986 to 2000. Indeed, Laurent et al. (1998) proposed different statistical criteria to validate the quality of satellite data compared to field data. For a reference v_i and estimation data set e_i comprising n values with $i = (1, n)$ whose mean is defined by $\overline{v}(\overline{e})$ and standard deviation by $\sigma_i(\sigma_e)$, the proposed criteria are the correlation coefficient, the bias, the RMSE (Root Mean Square Error) and the Nash index (**Table 2**). Also, the index of Nash measures a relative distance between the estimate and the reference. If $i = 1$, the estimate is perfect and if $i = 0$, the estimate equals the mean of the reference values (Arvor et al. 2008).

After validation, potential evapotranspiration (ETP) and the real evapotranspiration (ETR) were determined using Thornthwaite's method (Thornthwaite, 1954; Yao et al., 2015). The advantage of this method lies in the fact that it only asks for monthly temperatures and rainfall (N'Guessan Kouame et al., 2014). In this study, the reserve easily usable by plants (RFU) differs from north to south of the Marahoué basin. It is equal to a fraction of the RU (useful reserve) which is estimated by the development of the rooting of the vegetation (Biémi, 1992).

Table 2. Statistical test for validation of satellite data.

Statistical criterion	Equation
Correlation coefficient (R)	$R = \frac{\sum_{i=1}^{n}(v_i - \overline{v})(e_i - \overline{e})}{n\sigma_i\sigma_e}$
Bias (B)	$B = \overline{e} - \overline{v}$
$RMSE$ (Root Mean Square Error)	$RMSE = \sqrt{\frac{1}{n}\sum_{i=1}^{n}(e_i - v_i)^2}$
Nash index (I)	$I = 1 - \frac{RMSE^2}{\sigma_v^2}$

Since the Marahoué watershed is densely vegetated with strongly rooted soil in general, the *RFU* was determined according to Equation (15) (Combres et al., 1999; Khechana et al., 2019).

$$RFU = 2/3\,RU \tag{15}$$

The work of Sodexam (2012) specifies the values of the RU according to the climatic zones. Thereby:

- In the northern climatic zone, the *RU* = 30 mm (i.e. *RFU* = 20 mm), for the regions of Korhogo and Odienné;
- In the central and southern interior climatic zone, the *RU* = 60 mm (i.e. *RFU* = 40 mm), for the regions of bondoukou, Bouaké, Daloa, Man, Dimbokro, Yamoussoukro and Gagnoa;
- In the South-coastal climatic zone, the *RU* = 100 mm (i.e. *RFU* = 66.67 mm), for the regions of Adiaqué, Abidjan, Sassandra, San-pedro and Tabou.

Therefore, from the area of Séguéla and Mankono to Boundiali, we considered the *RFU* = 20 mm and from Bouaflé to Zuénoula the *RFU* = 40 mm. The month of November, which corresponds to the end of the rainy season in the basin, is taken as the starting point for the calculations.

The runoff (*R*) was determined by the empirical Tixéront-Berkaloff formula (Equation (16)) which uses the rainfall and the potential evapotranspiration calculated by the method of Thornthwaite (N'Guessan Kouame et al., 2014).

$$R = \frac{P^3}{3ETP^2} \tag{16}$$

R: runoff in mm;

P: average annual precipitation in mm;

ETP: average annual potential evapotranspiration calculated by the Thornthwaite method in mm.

Finally, the infiltration was determined from Equation (17) (Kouassi et al., 2007; N'Guessan Kouame et al., 2014).

$$I = P - \left(ETP + R\right) + \Delta S \tag{17}$$

With *P*: the depth of rain in millimeters (mm)

ETP: potential evapotranspiration (mm)

R: the stream of water (mm)

I: infiltration

ΔS: change in water stock

In this study, the variations in water stock (ΔS) are assumed to be zero. Because, on the scale of the annual hydrological cycle, the stock variations cancel each other out over a large basin (Mahé et al., 2005).

3. Results and Discussions

3.1. Conceptual Model of the Weathering Profile

3.1.1. Digital Terrain Model of the Marahoué Watershed

Few things stand out from the landscape of the Marahoué watershed. One no-

tices, in fact, a uniqueness and a flatness of the whole basin. It presents only small formations of hills by place not exceeding in general the 400 m of altitude. Indeed, the altitude increases slightly from south to north from 147 to 807 m. The highest areas are above the 9th parallel. That is to say the entire area located north of the town of Morondo (**Figure 5**). Tiered plateaus with a flat surface (horizontal or sub-horizontal) are common in some localities. According to Biémi (1992), this morphology promotes the formation of ponds, the infiltration of water and therefore the eventual recharge of the water tables.

3.1.2. Alterite Thickness

The roof of the basement has a slighthly uneven morphology in the Marahoué watershed. The dip of the basement is North-West, South-East and the altitudes are between 140 and 390 m (**Figure 6**). However, this dip of the basement roof does not seem to influence the distribution of the thickness of the alterites. It varies from place to place within the same area. Indeed, the analysis of the map of the thickness of the alterites obtained (**Figure 7**), shows that in the watershed of Marahoué, the thickness of the alterites varies between 0 and 80 m with an average of 26.72 m according to card statistics. We can therefore say that the average thickness of the alterites is high in the basin according to the Inter-State Hydraulic Committee (CIEH, 1978). Most of the thicknesses are between 0 and 40 m. The white areas correspond to the uninformed sectors of the map. This map also shows that the alterite layer is not continuous.

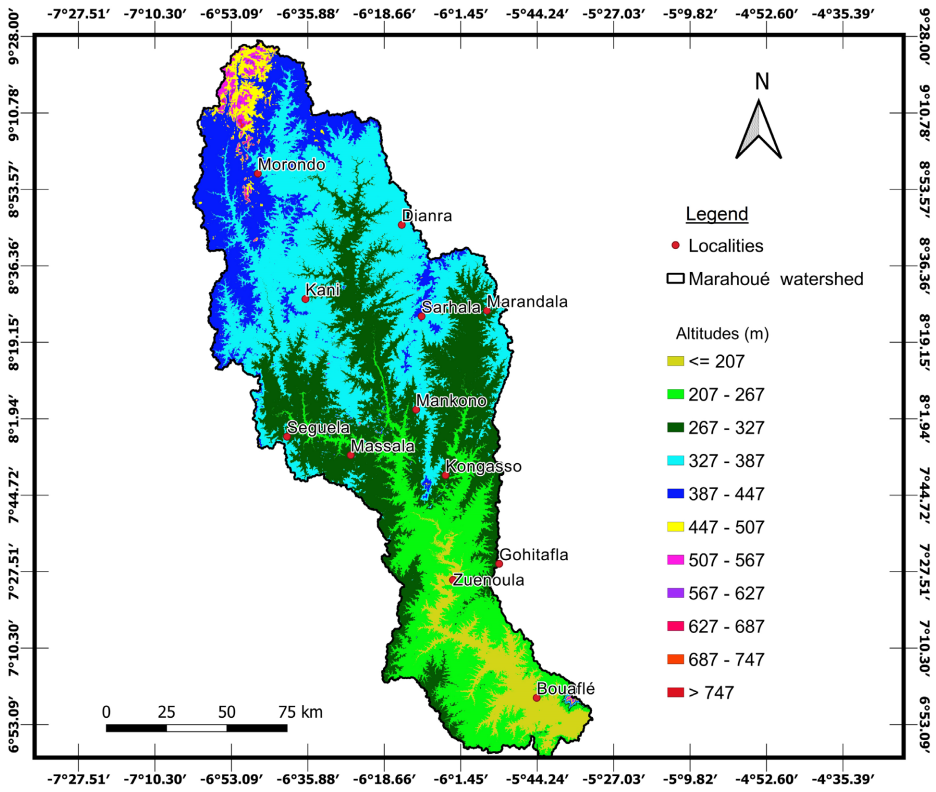

Figure 5. Digital terrain model of the Marahoué watershed.

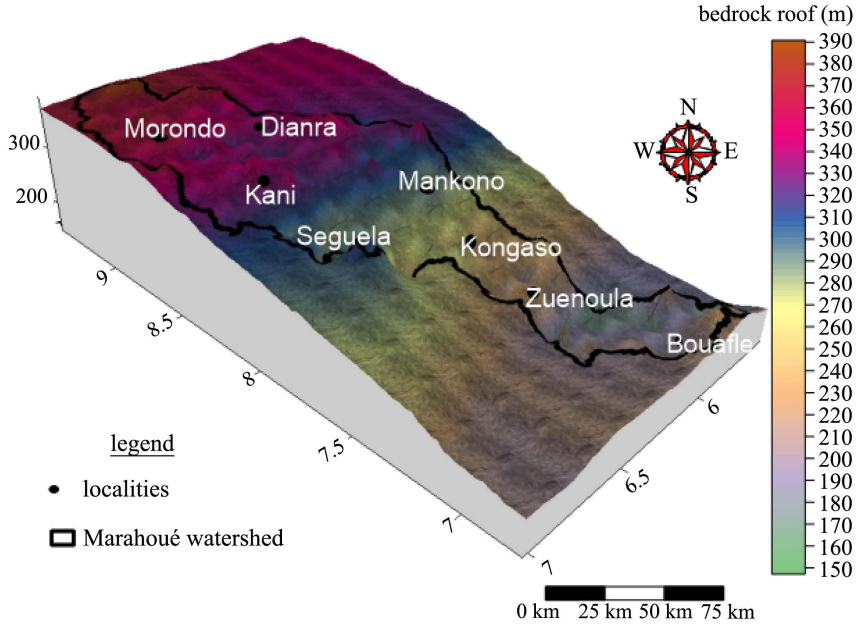

Figure 6. Map of the alterites/fissured medium interface.

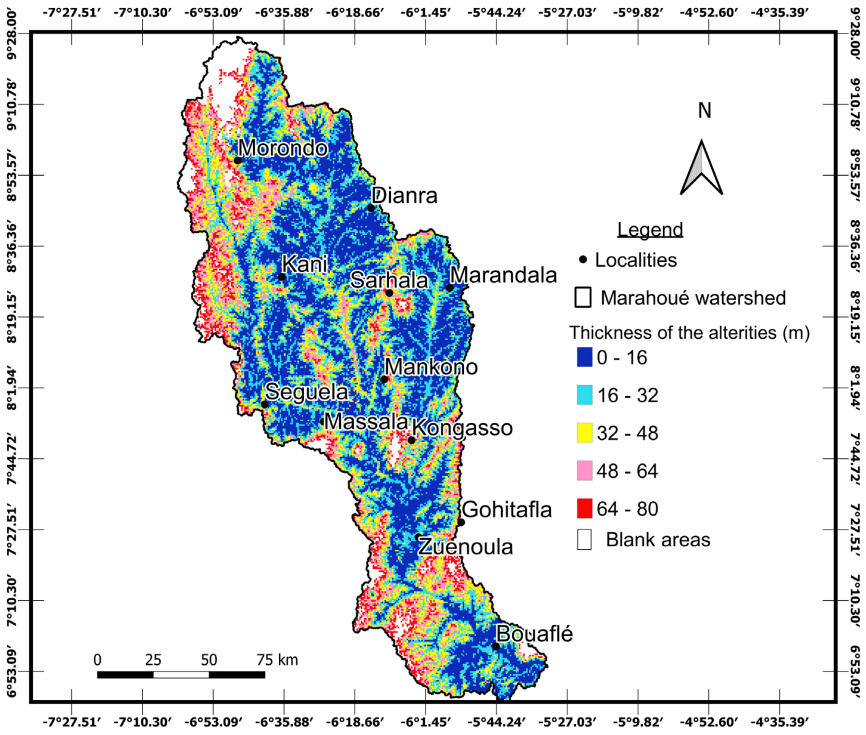

Figure 7. Alterite thickness map of the Marahoué watershed.

The fact that most of the thicknesses are between 0 and 40 m represents a significant advantage for the good productivity of the boreholes. In fact, studies have shown that beyond 60 m of alterite thickness, the productivity of boreholes becomes increasingly low in the basement zone (Koudou et al., 2016; Ble et al., 2015). According to Soro et al. (2010), hydraulically active fractures tend to close

with depth. They can become clogged if the arenas that cover them are clay.

3.1.3. Evaluation of the Linear Flow According to the Depth of the Borehole under the Base of the Unconsolidated Alterites

Figure 8 presents the results of the analysis of linear flows as a function of the depth of the boreholes below the base of the unconsolidated alterites (value denoted P). Analysis of this figure shows that the linear flows (Q/P) tend to decrease with depth. This is linked to the decrease in the number of cracks at depth. These results are consistent with the knowledge of basement hydrogeologists who have shown that the fissured horizon, located under the alterites, is the medium providing the best permeability of the subsoil and therefore the best instantaneous flows (Mougin et al., 2015). However, depending on the geological and hydrogeological environment, there is a depth beyond which the chances of finding an aquifer horizon decrease, particularly within altered basement rocks, due to the decrease in frequency and then the disappearance of permeable cracks (Dewandel et al., 2006).

3.1.4. Thickness of the Cracked Medium Producing the Best Flow Rates

After analysis of the 300 boreholes in the Marahouhé watershed (Figure 9), it appears that the thickness of the useful fissured horizon is 45 m with 8.45 m^3/h (0.187807556 $m^3/h/m \times 45$ m) as the flow rate of this fissured horizon useful.

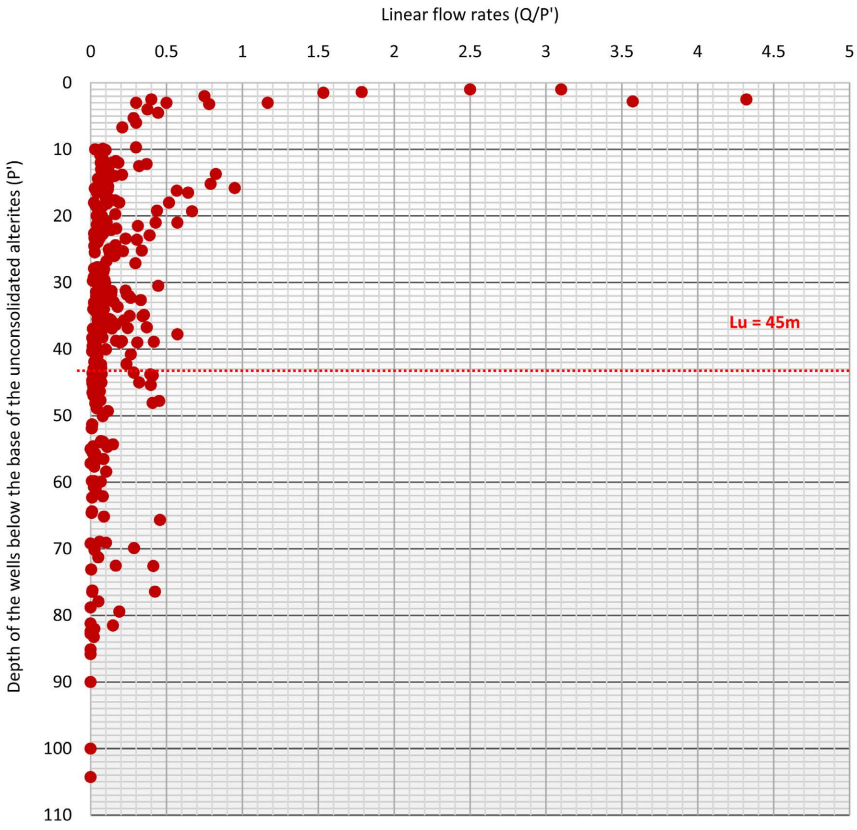

Figure 8. Linear flows as a function of borehole depth below the base of unconsolidated alterites.

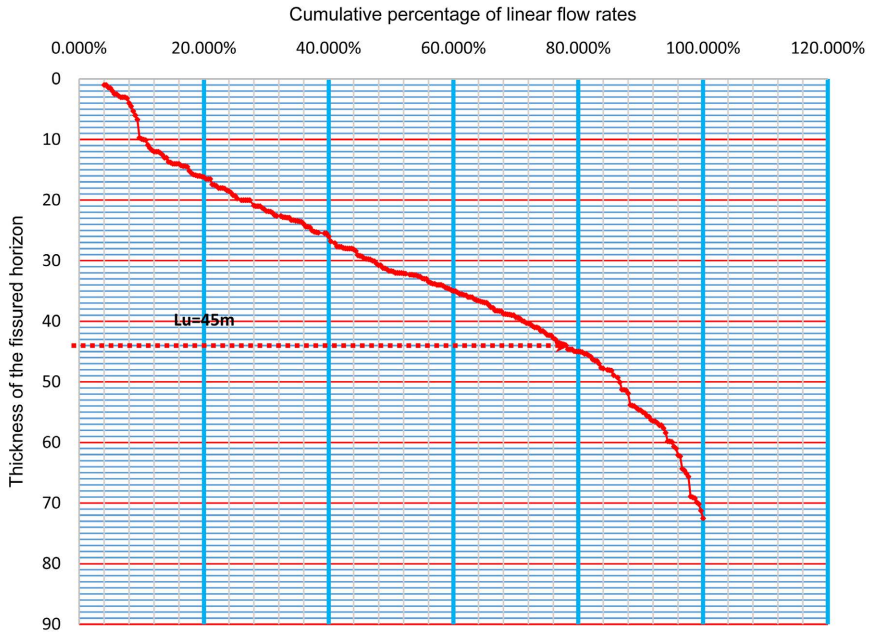

Figure 9. Statistical evaluation of the general thickness of the fissured horizon (here Lu = 45 m).

This useful thickness is comparable to that obtained in Brittany (44 m), during the work at Mougin et al. (2015).

3.1.5. Spatial Distribution of the Thickness of the Useful Fissured Horizon over the Basin

After statistical analysis of the boreholes carried out on these two geological formations (granites and shales), it appears that the thickness of the useful fissured horizon is 46.5 m, of which 9.42 m^3/h as flow at the level of the granites and 43 m with 6.42 m^3/h as useful flow associated with the level of the shales. This gives a useful, fairly small fissured horizon thickness range of between 43 and 47 m (**Figure 10**). Therefore, beyond these values, it is not useful to drill because of the high cost and the low throughput gain. This suggests that the "useful thickness" (at least as defined with the proposed method) is quite equivalent for the different lithologies in the Marahoué watershed. This range of useful thickness is greater than that obtained at the level of 27 geological formations in Burkina Faso, which varies between 25 m and 37 m (Courtois et al., 2008). On the other hand, it is lower than that obtained in Brittany (out of 83 geological formations) which varies from 19 to 65.7 m (Mougin et al., 2015).

3.1.6. Weathering Profile Layer Model

The different stratigraphic units were established from observations made during drilling. The longitudinal and transverse sections of the Marahoué watershed show that the different lithological horizons are not homogeneous throughout the basin (**Figure 11** and **Figure 12**). There is also a strong accumulation of alterites in the valleys, while these tend to disappear on the slopes. The fissured horizon remains substantially unchanged over the entire basin and outcrops in places.

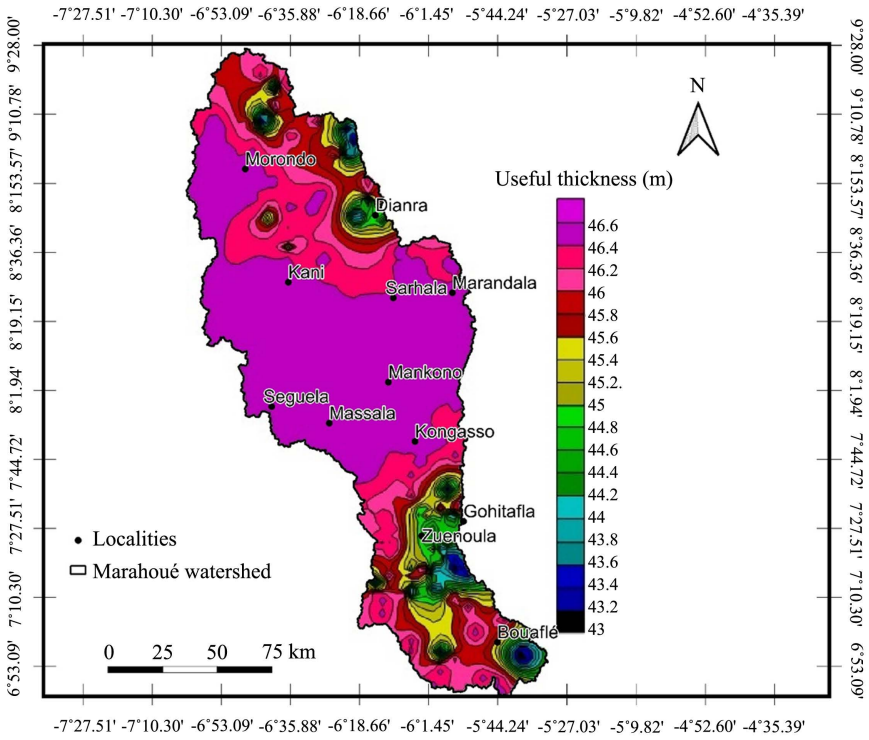

Figure 10. Marahoué watershed, defined by the method of 80% of the cumulative linear flows.

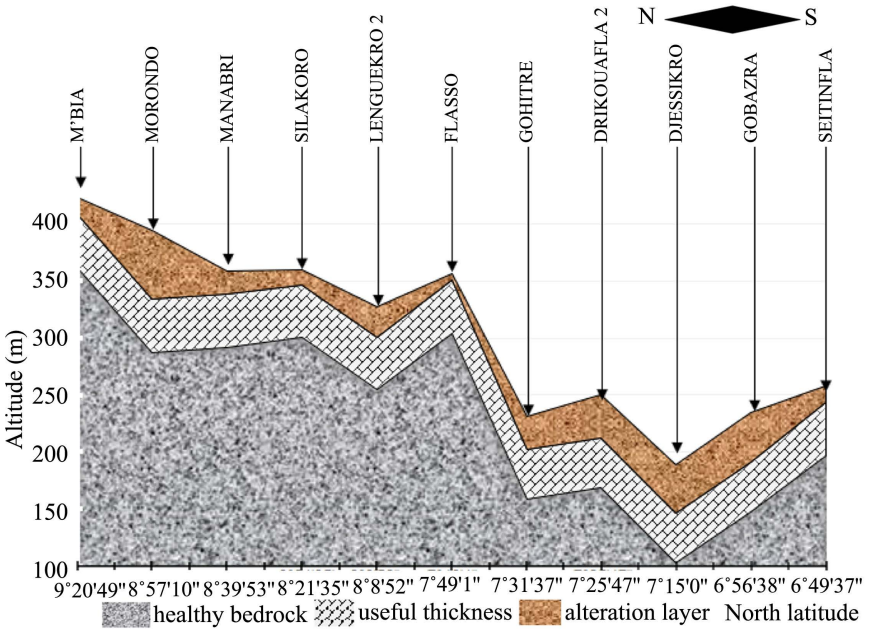

Figure 11. Marahoue watershed conceptual layer model in N-S direction.

3.2. Hydrodynamic Parameters of the Marahoué Watershed

The porosities determined at the Marahoué watershed are relatively low. They vary from 0.16% to 5.37%, the maximum of which is reached in the village of Séitinfla near Bouaflé. The maximum value of the porosity obtained in the basin

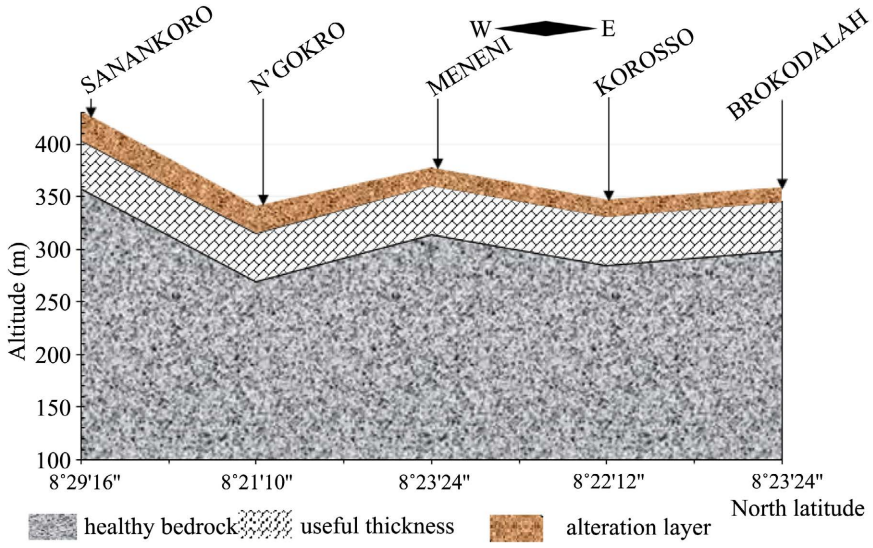

Figure 12. Marahoue watershed conceptual layers model in W-E direction.

is higher than that encountered in the literature (2% at the level of fissured granites and schists) (Fouché, 2013). However, it demonstrates that certain areas of the basin are sufficiently fractured and therefore capable of being assimilated to a homogeneous medium (Thiery et al., 1982).

The majority of transmissivities are moderately high (59.62%). In addition, 78.85% of the transmissivity belong to the middle and strong classes. The highest transmissivity (3.3110E−03 m^2/s) in the Marahoué basin was obtained in the village of Drikouafla 2 in the sub-prefecture of Zuenoula. However, the lowest transmissivity (2.3242E−06 m^2/s) was recorded at Gbénan in the Séguéla sub-prefecture. We deduce from this analysis that the transmissivity of at the level of the Marahoué watershed is clearly good (CIEH, 1978).

The permeabilities obtained vary from 6.640×10^{-08} to 2.255×10^{-04} m/s with an average of 8.95493×10^{-06} m/s. This means that the permeability at the level of the marahoué watershed is of poor quality. Thus, the aquifers crossed by the various boreholes are semi-permeable types (Castany, 1982). Finally, the determined storage coefficients vary between 4.51×10^{-05} at 2.93×10^{-03}. The maximum was obtained at Manabri in the Kani sub-prefecture. Indeed, the minimum storage coefficient is less than 10^{-02}, which means that the aquifers crossed by the various boreholes are confined or semi-confined (Soro, 2017).

3.3. Piezometric Analysis

The piezometric map (**Figure 13**) gives an overview of groundwater flow dynamics from fissured aquifers in the Marahoué watershed. In general, all groundwater flows towards the basin outlet. That is to say the North-West – South-East direction. There are areas of possible recharge of the basin's aquifers in places. These zones are factors for good borehole productivity because confined and semi-confined aquifer systems usually have specific recharge zones where the aquifer outcrops (Soro, 2017).

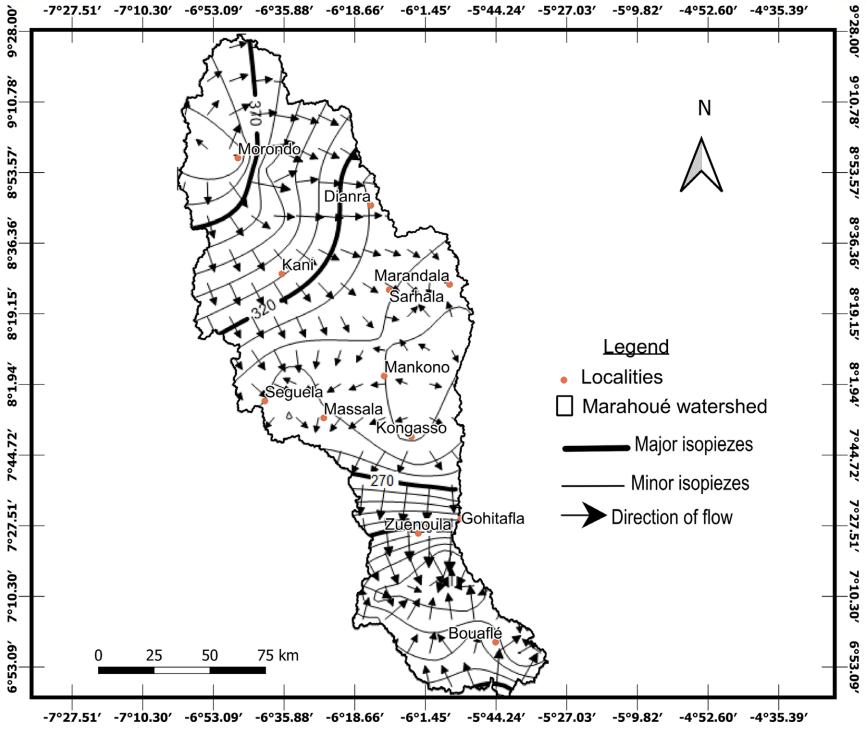

Figure 13. Piezometric map of the Marahoué watershed for the month of January 1999.

3.4. Validation of Satellite Data

There is a very strong correlation between terrestrial data and satellite data (Figure 14 and Table 3). This correlation varies from 0.94 to 0.98. The Nash index also varies from 0.64 to 0.85. These values indicate that the NASA-power estimates are good. Therefore, these satellite data are likely to be used for the calculation of the hydrological balance. These good correlations are in line with the results of several authors in West Africa and Brazil (Guillo, 1996; Arvor et al., 2008; Gascon, 2016). These authors demonstrated that there is good spatial coherence of interannual rainfall at monthly and seasonal time steps.

3.5. Hydrological Balance of the Marahoue Watershed

Marahoué watershed corresponds to the zone where the infiltration is the highest. The infiltration rate in this area during the period 1986 to 2017 varies between 250 and 460 mm (Figure 15). The Bouaflé sector, located at the outlet of the basin, recorded the lowest amount of infiltrated water (250 mm on average, or 19.92% of the amount of precipitated water). This low infiltration obtained at Bouaflé is greater than that obtained at Yamoussokro from 1975 to 2001 (70 mm or 6.15% of the precipitated water layer) (N'Guessan Kouame et al., 2014). These results are substantially equal to those of the work of Irié (2019).

3.6. 3D Model of the Weathering Profile

In sum, the conceptual model of the weathering profile takes into account three stratigraphic units with different properties (Figure 16). The first layer corresponds

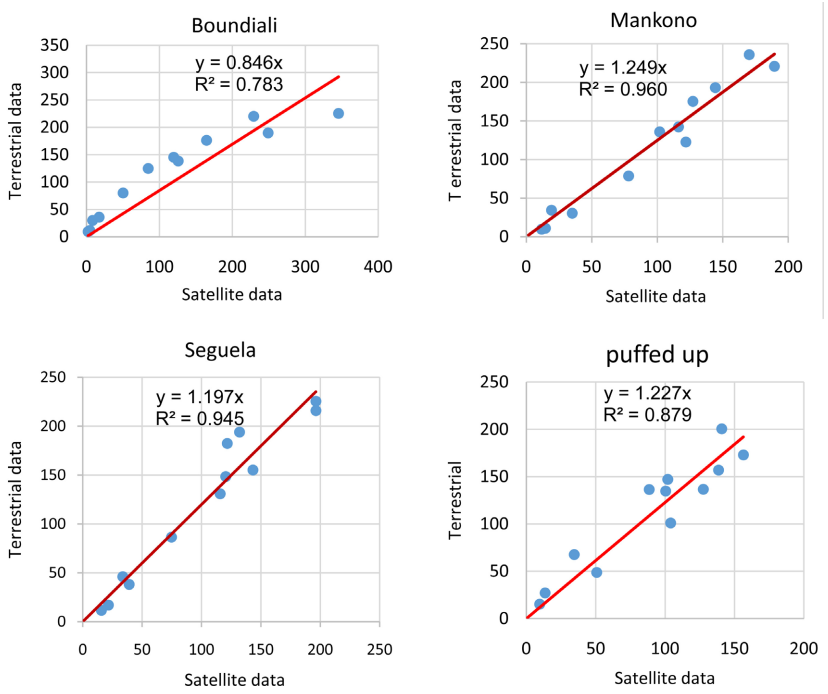

Figure 14. Relationship between terrestrial and satellite data.

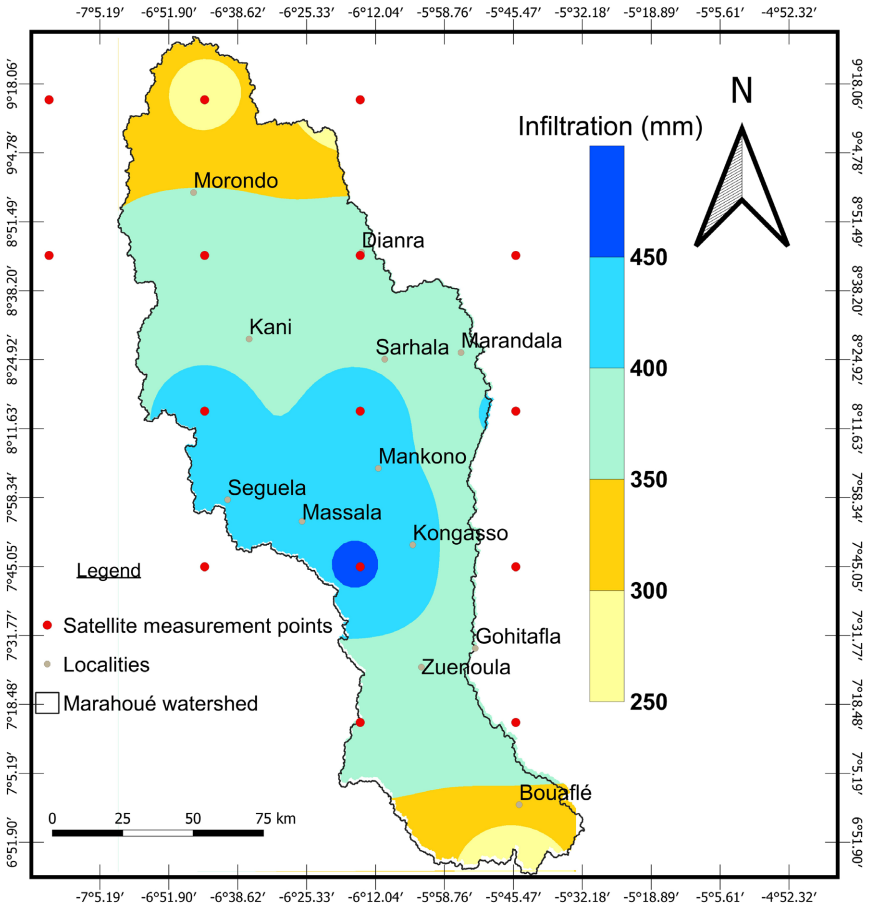

Figure 15. Variation of infiltration in the Marahoué watershed.

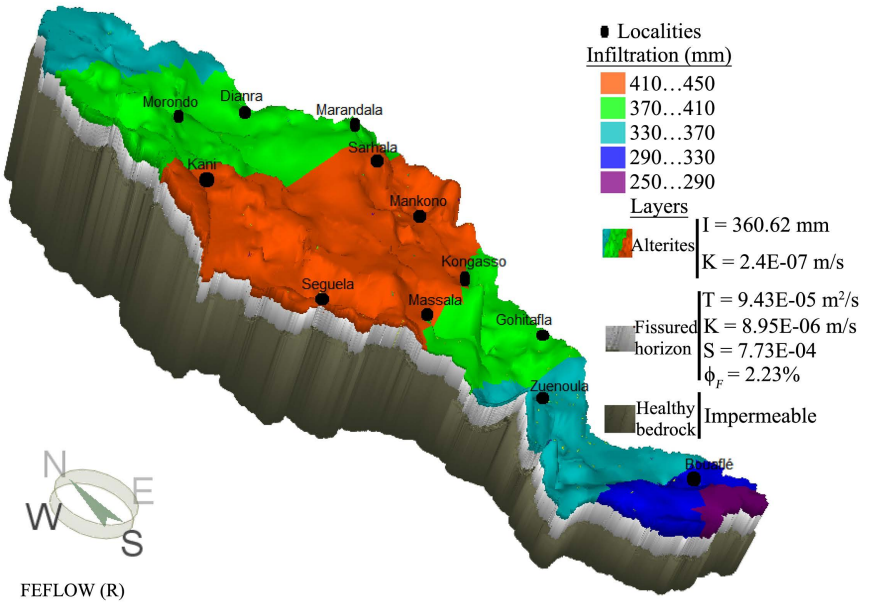

Figure 16. Simplified stratiform model of the hydrogeological structure of the aquifers of the Marahoué watershed.

Table 3. Validation of satellite data.

	MUFFLE	BOUNDIALI	MANKONO	SEGUELA
R	0.96	0.94	0.98	0.97
RMSE	30.40	43.23	31.79	29.16
Deviation	50.56	111.87	61.98	63.65
Nash	0.64	0.85	0.74	0.79

to alterites. It varies from 0 to 80 m. It can be noted that this thickness is not specific to a geographical area of the basin. Indeed, due to their clay content, alterites are characterized by low water permeability (2.4×10^{-7} m/s on average at basin level). Nevertheless, they have significant storage capacities. Their piezometric levels drop significantly in the dry season and rise again in the rainy season (Biémi, 1992). This causes wells to dry up during dry seasons. The second layer is that of the fissured horizon. Its thickness varies from 43 to 47 m according to the geological layers with an average equal to 45 m. Beyond these values, the chance of obtaining hydraulically active fractures decreases. In addition, this part encloses the hydraulically active fissures of the basin. The frequency of these cracks decreases steadily from top to bottom (Yao, 2011). According to Dewandel et al. (2006), most of the permeability of basement aquifers comes from the lower part of the weathering profile (the stratiform fissured horizon) which is located under the unconsolidated alterites (when these have not been eroded). The last layer corresponds to the sound base. This is unweathered bedrock. Apart from fractures of tectonic origin that may exist locally, this bedrock offers only a very low underground water storage capacity (Lachassagne et al., 2005).

Given its infinite nature, it was limited to an altitude of 80 m during the design of the model.

4. Conclusion

The implementation of the conceptual model of groundwater flows in the Marahoué watershed has made it possible to characterize the weathering profile. This profile consists of three stratigraphic layers (alterites, fissured horizon and sound basement). The thickness of the alterites varies from 0 to 80 m. That of the useful fissured horizon is between 43 and 47 m. Then, the analysis of the hydrodynamic parameters made it possible to know that the different aquifers are confined or semi-confined. Groundwater generally flows towards the outlet of the basin, i.e. in the North-West - South-East direction. This work has contributed to the improvement of knowledge of fissured aquifers by proposing a multidisciplinary method, adaptable to any analogous system, and offering valuable assistance for a reasoned management of groundwater resources. However, further research is needed to best facilitate the exploitation of this resource. Thus, in the future, it will be necessary to carry out a steady-state simulation to better understand the direction of groundwater flow. Then perform a transient simulation to determine the influence of climate variability and abstraction on flows, the relationship between aquifers and surface water. In addition, set up a global management model for groundwater resources for its quantitative and qualitative sustainability at the level of the marahoué watershed.

Conflicts of Interest

The authors declare no conflicts of interest regarding the publication of this paper.

References

Akpo, K. S., Coulibaly, L. S., Coulibaly, L., & Savane, I. (2016). Temporal Evolution of the Use of Pesticides in Tropical Agriculture in the Marahoué Watershed, Côte d'Ivoire. *International Journal of Innovation and Applied Studies, 14,* 121-131.

Anderson, M., & Woessner, W. W. (1992). *Applied Groundwater Modelling: Simulation of Flow and Advective Transport* (381 p). Academic Press.

Arvor, D., T Dubreuil, V., Ronchail, J., & Simões Penello Meirelles, M. (2008). Contribution of TRMM Data 3B42 Has the Study of Precipitation in Mato Grosso. *Climatologie, 5,* 21 p.

Assemian, A. E. (2014). *Study of Groundwater Potential in the Department of Bongouanou (Centre-East of Côte d'Ivoire) by Remote Sensing and GIS* (223 p). Doctoral Thesis, Félix Houphouet University.

Avenard, J. M., Eldln, M., Girard, M., Sircoulon, J., Touchebeuf, P., Guillaumet, J. L., Adjanohoun, E., & Perraud, A. (1971). *The Natural Environment of the Ivory Coast* (400 p). Office of Scientific and Technical Research Overseas.

Baron, C., & Bonnassieu, A. (2011). The Challenges of Access to Water in West Africa: Diversity of Modes of Governance and Conflicts of Use. *Developing Worlds, No. 156,* 17-32. https://doi.org/10.3917/med.156.0017

Barthélemy, Y., & Seguin, J. J. (2016). *Mesh Modeling of Underground Flows – Principles, Approach and Recommendations.* Final Report. BRGM/RP-62549-FR, 140 p., 50 ill., 2 tabl., 3 Years.

Biémi, J. (1992). *Contribution to the Geological, Hydrogeological and Remote Sensing Study of the Sub-Sahelian Watersheds of the Precambrian Basement of West Africa: Hydrostructural, Hydrodynamic, Hydrochemistry and Isotopy of Discontinuous Aquifers of Furrows and Granite Areas of Haute Marahoué (Ivory Coast)* (480 p). State Thesis, Univ. Abidjan, Ivory Coast.

Ble, L. O., Ake, S. T., Etienne, G., Ahoussi, E. K., Oga, M. S., Biémi, J., & Akossi, D. (2015). Productivity of Water Wells in Crystalline and Crystallophyllian Environment in Daoukro Region (Center-East of the Ivory Coast). *Synthese, 30,* 76-90, 15 p.

Boudevillain (2003). *Contribution to the Definition of the Characteristics of an Urban Hydrological Radar Very Short-Term Rain Forecast* (169 p). Thesis to Obtain the Degree of University Doctor BLAISE PASCAL.

Inter-African Hydraulic Studies Committee (Comite Interafricain D'etudes Hydrauliques (CIEH)) (1978). Method of Study and Research of Groundwater in the Crystalline Rocks of West Africa. *Geohydraulics, 2,* 204 p.

Carter, R. C., & Parker, A. (2009). Climate Change, Population Trends and Groundwater in Africa. *Hydrological Sciences Journal, 54,* 676-689. https://doi.org/10.1623/hysj.54.4.676

Castany, G. (1982). *Principle and Method of Hydrogeology* (237 p). Dunod University.

Combres, J. C., Le Mezo, L., Mete, M., & Bourjon, B. (1999). Useful Reserve and Humidity Measurements. Difficulty in Calibrating Water Balance Models. *Agriculture and Development, 24,* 39-47.

Cooper., H. H., & Jacob, C. E. (1946). A Generalized Graphical Method for Evaluating Formation Constants and Summarizing Well Field History. *Eos, Transactions American Geophysical Union, 27,* 526-534. https://doi.org/10.1029/TR027i004p00526

Courtois, N., Lachassagne, P., Wyns, R., Blanchin, R., Bougaïré, F. D., Somé, S., & Tapsoba, A. (2008) Country-Scale Hydrogeological Mapping of Hard-Rock Aquifers and Its Application to Burkina Faso. *Groundwater, 48,* 269-283. https://doi.org/10.1111/j.1745-6584.2009.00620.x

Delor, C., Simeon, Y., Vidal, M., Zeade, Z., Kone, Y., & Adou, M. (1995). *Geological Map of Côte d'Ivoire at 1/200,000, Séguéla Sheet* (19 p). Memorandum No. 9, Department of Mines and Geology.

Dewandel, B., Lachassagne, P., Wyns, R., Maréchal., J., & Krishnamurthy, N. C. (2006). A Generalized 3-D Geological and Hydrogeological Conceptual Model of Granite Aquifers Controlled by Single or Multiphase Weathering. *Journal of Hydrology, 330,* 260-284. https://doi.org/10.1016/j.jhydrol.2006.03.026

Duran, V. (2005). *Multidisciplinary Research to Characterize Two Fractured Aquifers: The Mineral Waters of Plancoët in a Metamorphic Context, and of Quezac in a Carbonate Environment* (302 p). Doctoral Thesis, University Paris VI.

Durand, V., Léonardi, V., De Marsily, G., & Lachassagne, P. (2015). The Two-Layer Conceptual Model of Hard-Rock Aquifers: Validation with a Deterministic Hydrogeological Model. In 20*th Technical Days of the International Association of Hydrogeologists* (French Chapter, 129 p.). ICES Auditorium.

Faillat, J. P., Somlette, L., Jegat, S., Le Jeune, C., & Vasquez, M. (1998). *Determination of the Hydrodynamic Parameters of the Fissured Schisto-Sandstone Aquifer of the Experimental Perimeter of Kerveldréach*. Final Report Watershed and Transmission of Pollution Program on the Coastline. IFREMER-DERO.OELO2598.

Fouché, O. (2013). Aquifers, Aquifers and Water Tests. In Th. Kremer, & C. Plumelle (Eds.), *Théorie et pratique de la géotechnique* (pp. 725-848). Editions du Moniteur. https://www.researchgate.net/publication/278801957

Gascon, T. (2016). *Impact of Spatial and Temporal Resolution of Rainfall Inputs for Hydrological Modeling in West Africa and Implication in the Use of Satellite Products. Case Study on the Ouémé Basin in Benin* (239 p). Doctoral Thesis Grenoble Alpes University Community.

Goula, B. T. A., Savane, I., Konan, B., Fadika, V., & Kouadio, G. B. (2006). Impact of Climate Variability on the Water Resources of the N'zo and N'zi Basins in Côte d'Ivoire (Humid Tropical Africa). *Vertigo, No. 1,* 1-12.

Guillo, B. (1996). *Methods for Estimating Precipitation by Satellite: The EPSAT Network and the Problems of Research, Transfer and Validation.* https://horizon.documentation.ird.fr/exldoc/pleins_textes/pleins_textes_6/colloques2/010008086.pdf

Irie, G. R., Soro, G. E., & Goula Bi, T. A. (2016). Recent Spatio-Temporal Variations of Parameters Rainfall and Their Impact on the Flow of the Marahoué River (Ivory Coast). *Larhyss Journal, No. 25,* 241-258.

Irié, G. R. (2019). *Impacts of Climate Change on Water Resources in the Marahoué Watershed (Côte d'Ivoire)* (190 p). Doctoral Thesis, Nangui University Abrogoua.

Irie, G. R., Soro, G. E., & Goula Bi, T. A. (2015). Changes in Surface Conditions and Spatio-Temporal Evolutions of Precipitation in the Marahoué Watershed (Côte d'Ivoire). *International Journal of Innovation and Applied Studies, 13,* 386-397.

Jaunat, J. (2013). *Characterization of Groundwater Flows in Fissured Media Using a Coupled Hydrology-Geochemistry-Hydrodynamics Approach Application to the Ursuya massif (Basque Country., France)* (343 p). Doctoral Thesis, University of Bordeaux 3.

Kamagate, B., Gone, D. L., Doumouya, I., Ouattara, I., Ouedraogo, M., Bamba, A., & Savane, I. (2011). Groundwater-River Relationship in the Bandama Watershed in the Middle of a Fissured Bedrock in Côte d'Ivoire: Coupled Hydrochemistry—Remote Sensing Approach. *International Journal of Biological and Chemical Sciences, 5,* 206-216. https://doi.org/10.4314/ijbcs.v5i1.68099

Khechana, S., Ghomri, A., Mani, M., Djedid, T., & Miloudi, A. (2019). *Contribution to the Identification of the Easily Usable Reserve (RFU) in Arid Regions (Case of the Oued Valley Suf).* https://dspace.univouargla.dz/jspui/bitstream/123456789/24449/1/Salim%20KHECHANA_2.pdf

Koffi, K. (2004). *Contribution to the Study of Coupled Hydrogeochemical Processes in Mining Waste Stocks: The Case of the Carnoules Site (Gard., France)* (161 p). Doctoral Thesis, University of Montpellier II.

Koïta, M. (2010). *Characterization and Modeling of the Hydrodynamic Operation of a Fractured Aquifer in the Bedrock Zone. Dimbokro-Bongouanou Region (Central East of Côte d'Ivoire).* Doctoral Thesis, University of Montpellier II.

Kouamé, K. I. (2007). *Physico-Chemical Water Pollution in the Akouédo Landfill Area and Analysis of the Risk of Contamination of the Abidjan Aquifer by a Model Simulating the Flow and Transport of Pollutants* (229 p). Unique Doctoral Thesis, University of Abobo-Adjamé.

Kouassi, A. M., Okaingni, J. C., Kouakou, K. E., & Biemi, J. (2013). Evaluation of the Hydraulicproperties of Crystalline and Crystallophyllian Basement Aquifers: Case of the N'zi-Comoé Region (Centre-East of Côte d'Ivoire). *International Journal of Innovation*

and AppliedStudies, 2, 61-71.

Kouassi, A. M., Kouame, K. F., Saley, M. B., & Yao, B. K. (2007). Identification of Trends in the Rain-Flow Relationship and Aquifer Recharge in a Context of Hydroclimatic Variability: Case of the N'zi (Bandama) Watershed in Côte d'Ivoire. *European Journal of Scientific, 16,* 412-425.

Koudou, A., N' dri, B. E., Niamke, N. H., Adjiri, O. A., Sombo, A. P., & Niangoran, K. C. (2016). Productivity Analysis and Estimation of Vulnerability to Pollution for Optimizing the Location of Boreholes in Bedrock Aquifers of the N'zi Watershed (Côte d'Ivoire). *Bulletin of the Scientific Institute, Rabat, Earth Sciences Section, 38,* 149-164.

Lachassagne, P., Dewandel, B., & Wyns, R. (2015). The Hydrogeological Conceptual Model of Weathered Basement Aquifers and Its Practical Applications. In La Roche-sur-Yon, *Proceedings of the Conference "Basement Aquifers: Update on Concepts and Operational Applications. Twentieth Technical Days of the French Hydrogeology Committee of the International Association of Hydrogeologists* (11 p).

Lachassagne, P., Maréchal, J. C., Sahmed, S. H., Dewandel, B., Gandolfi, J. M., Krishnamurthy, N. S., Subrahmanyam, K., & Wyns, R. (2005). New Tools and Methods to Manage and Protect Groundwater Resources in Basement Regions. *Hydroplus, No. 150,* 4 p.

Laurent, H., Jobard, I., & Toma, A. (1998). Validation of Satellite and Ground-Based Estimates of Precipitation over the Sahel. *Atmospheric Research, 47-48,* 651-670. https://doi.org/10.1016/S0169-8095(98)00051-9

Mahé, G., L'Hotte, Y. Olivry, J. C., & Wotling, G. (2001). Trends and Discontinuities in Rainfall of West and Central Africa: 1951-1989. *Hydrological Sciences Journal, 46,* 211-226. https://doi.org/10.1080/02626660109492817

Mahé, G., Paturel, J. E., Servat, E., Conway, D., & Dezetter, A. (2005). The Impact of Land Use Change on Soil Water Holding Capacity and River Flow Modeling in the Nakambe River, Burkina Faso. *Journal of Hydrology, 300,* 33-43. https://doi.org/10.1016/j.jhydrol.2004.04.028

Mougin, B., Dheilly, A., Thomas, E., Blanchin, R., Courtois, N., Lachassagne, P., Wyns, R., Allier, D., & Putot, E. (2015). Regional Mapping at 1/250,000 of the Thickness of Alterites and the Useful Fissured Horizon (SILURES Bretagne Project). *Basement Aquifers: Update on Concepts and Operational Applications: 20th CFH and IAI Days*, La Roche-sur-Yon.

N'Guessan Kouame, A., Kouassiamani, M., Gnaboa, R., Traoré, K. S., & Houenou, P. V. (2014) Analysis of Hydrological Phenomena in an Urbanized Watershed: Case of the City of Yamoussoukro (Central Ivory Coast). *Larhyss Journal, 17,* 135-154.

Ouedraogo, M. (2016). *Characterization of Basement Aquifers for the Improvement of the Productivity of Village Hydraulic Boreholes in the Watershed of the Upstream Bandama Blanc (Northern Côte d'Ivoire)* (241 p). Doctoral Thesis, Paris-Saclay University.

Savané, I., Goze, B. B., Hugh, Q., & Gwyn, J. (1997). Evaluation of the Productivity of Works in the Basement by the Study of Fractures and the GIS in the North-West Region of Côte d'Ivoire. *Hard Rock Hydrosystems (Proceedings of Rabat Symposium S2), 241,* 9 p.

Soro, D. D. (2017). *Characterization and Hydrogeological Modeling of an Aquifer in the Middle of a Fractured Bedrock: Case of the Sanon Experimental Site (Central Plateau Region in Burkina Faso)*. Thesis Jointly Supervised by the Pierre and Marie Curie-Paris 6 University (UPMC) and the International Institute for Water and Environmental Engineering (2iE).

Soro, G., Soro, N., Ahoussi, K. E., Lasm, T., Kouame, F. K., Soro, T. D., & Biemi, J. (2010).

Evaluation of the Hydraulic Properties of Fractured Aquifers of Crystalline and Metamorphic Formations in the Lacs Region (Central Côte d'Ivory). *Studies Geologicos, 66,* 227-242.

Suski, B. (2006). *Characterization and Monitoring of Water Flows in Porous Media Using the Spontaneous Potential Method* (202 p). Doctoral Thesis, University of Law, Economics and Sciences of Aix-Marseille III.

Sodexam (2012). *Bulletin Agrometeorologique Decadaire*. http://www.wamis.org/countries/cdivoire/cdivr2012121.pdf

Thiery, D., Vandenbeusch, M., & Vaubourg, P. (1982). *Interpretation of Test Pumping in a Fissured Aquifer Medium* (69 p). Report from BRGM 82 SGN 920 EAU, BRGM (Bureau de Recherches Géologiques et Minières).

Thornthwaite, C. W. (1954). An Approach toward a Rational Classification of Climate. *Transaction American Geophysics Union, 27,* 5-99.

Yao, A. B., Kouame, K. I., Kouassi, K. A., Koffi, K., Goula, B. T. A., & Savane, I. (2015). Estimation of the Recharge of a Coastal Aquifer in the Humid Tropical Zone: Case of the Aquifer of the Continental Terminal of Abidjan (Côte d' Ivory). *International Journal of Innovation and Applied Studies, 12,* 888-898.

Yao, K. T. (2011). *Hydrodynamics in Crystalline and Crystallophyllian Basement Aquifers in the South-West of Côte d'Ivoire: Case of the Department of Soubré: Contributions of Remote Sensing, Geomorphology and Hydrogeochemistry* (339 p.). Doctoral Thesis, National Conservatory of Arts and Crafts and the University of Cocody.

Annex

Table of symbols and their meanings

Symbols	MEANINGS	Units
L_u	The thickness of the useful cracked horizon	m
Q_{Lu}	The flow rate of this useful fissured horizon	m^3/s
Q_{pl}	The flow rate of the useful fissured medium	m^2/s
Q/P'	the instantaneous linear flow	m^2/s
Nf	The number of boreholes	unitless
ϕ_F	Porosity of fractures and connected pores	unitless
C_e	Water compressibility coefficient	$m^3/m^3/bar$
C_{ma}	Matrix compressibility coefficient.	$m^3/m^3/bar$
T	Transmissivity	m^2/s
s'	Continuation of the recording of the drawdown in the control piezometer	m
Q	Pumping flow rate value that created the initial drawdown	m^3/s
t	Time elapsed from the start of pumping until it stops	s
t'	Time counted after this stop	s
S	The storage coefficient	unitless
e	The thickness of the aquifer	m
ρ_w	Density of water	kg/m^3
g	gravitational acceleration	m/s^2
K	The Hydraulic conductivity	m/s
Np	The piezometric level referring to the edge of the casing	m
Z_{TN}	The altitude of the natural terrain at the location of the structure	m
N_{mesure}	The depth of the water surface measured with the probe	m
H_d	The height (m) of the casing above ground	m
$RMSE$	Root Mean Square Error	unitless
$\overline{v}(\overline{e})$	The mean	unitless
$\sigma_i(\sigma_e)$	standard deviation	unitless
I	The index of Nash	unitless
R	Correlation coefficient	unitless
ETP	Potential evapotranspiration	mm
ETR	The real evapotranspiration	mm
RFU	The reserve easily usable	mm

Continued

R	Runoff	mm
P	Average annual precipitation	mm
I	Infiltration	mm
ΔS	Change in water stock	mm